Supporting Information

Korendovych et al. 10.1073/pnas.1018191108

SI Text

NMR Data Collection and Analysis. All NMR spectra were recorded at 20 °C on a Bruker DMX-600 spectrometer equipped with a 5-mm x,y,z-shielded pulsed-field gradient triple-resonance probe except simultaneous 3D $^{15}N/^{13}C^{aliphatic}/^{13}C^{aromatic}$-resolved [$^1H$, ^1H] NOESY (1) collected on a Varian INOVA 600 spectrometer equipped with cryogenic probe. The standard through-bond correlated NMR experiments (2) were collected for backbone and side chain resonance assignment. 3D NOESY spectra with different mixing times were acquired to confirm/extend assignments and derive ^1H-^1H distance constraints. $^1D_{NH}$ RDCs were measured using a ^1H-^{15}N IPAP-HSQC experiment (3) with Pf1 phage (approximately 25 mg/mL) as the alignment medium (4). Spectra were processed and analyzed with the programs NMRPipe (5), Sparky (T.D. Goddard and D.G. Kneller, UCSF) and XEASY (6). Proton chemical shifts were referenced to residual water signal, ^{13}C and ^{15}N chemical shifts were referenced indirectly.

Resonance Assignments. Sequence specific backbone ($^1H^N$, ^{15}N, $^1H^\alpha$, $^{13}C^\alpha$) and $^1H^\beta$ / $^{13}C^\beta$ resonance assignments were obtained by using HNCA, HN(CO)CA, HNCO, HNCACB, and CACB (CO)NH experiments. Side chain chemical shifts were assigned with H(CCO)NH, C(CO)NH, aliphatic HCCH-COSY, HCCH-TOCSY, and CCH-TOCSY. Assignments were confirmed and extended by 3D ^{15}N-resolved [^1H, ^1H]-NOESY (mixing time: 200 ms), 3D $^{13}C^{aliphatic}$-resolved [^1H, ^1H]-NOESY(mixing time: 150 ms), and 3D $^{13}C^{aliphatic}$-resolved [^1H, ^1H]-NOESY (mixing time: 150 ms). Overall, assignments were obtained for 99% of the backbone (excluding a portion of the expression tag) and $^{13}C^\beta$, and for 98% of the side chain chemical shifts (excluding Lys NH_3^+, Arg NH_2, OH, side chain ^{13}CO and aromatic $^{13}C^\gamma$) assignable with the set of NMR experiments provided above. Chemical shifts were deposited in the BioMagResBank (7) (accession code 16994).

Structure Calculations. ^1H-^1H upper distance limit constraints for structure calculations were extracted from simultaneous 3D $^{15}N/^{13}C^{aliphatic}/^{13}C^{aromatic}$-resolved [$^1H$, ^1H] NOESY (mixing time: 100 ms). Backbone dihedral angle constraints were obtained using the program TALOS+ (8) for residues located in well-defined secondary structure elements. Assignment of long-range NOEs was done semiautomatically with CYANA (9). Ca^{2+} ligation was treated as distance restraints with the ligating atoms as in the X-ray structure of CaM (PDB ID code 1CLL) (10). The final structure was calculated by simulated annealing in torsion angle space using the XPLOR-NIH program (11). First, an approximate structure was calculated by slowly cooling an extended structure from 3,000 K to 20 K with NOE and backbone dihedral restraints. The final parameters in the simulated annealing target function are: 1,000 kcal mol^{-1} Å^{-2} for bond lengths; 500 kcal mol^{-1} rad^{-2} for angles and improper dihedrals; 4 kcal mol^{-1} Å^{-4} for the quartic van der Waals repulsion term; 30 kcal mol^{-1} Å^{-2} for distance restraints; 200 kcal mol^{-1} rad^{-2} for dihedral angle restraints. A total of 50 structures were calculated and the lowest energy structure was selected as a starting structure for further refinement with addition of RDCs. 50 $^1D_{NH}$ RDCs of well-defined secondary structure elements were fitted the lowest energy NOE-derived structure to calculate the axial and rhombic components of the alignment tensor by the singular value decomposition method using PALES (12). Then distance and dihedral angle constraints together with 40 (80%) randomly selected RDCs were used to refine the structure. Of 100 calculated structures, 20 lowest energy structures were chosen as an ensemble to represent the solution structure. Ramachandran statistics for all the residues excluding the His tag (68–148): most favored regions −93.4%; additional allowed regions −4.9%; generously allowed regions −1.2%; disallowed regions −0.5%. All observed outliers belong to the residues in the flexible linker regions. The NMR and refinement statistics are summarized in Tables S2 and S3.

Product Characterization. The product of the reaction catalyzed by AlleyCat was characterized by 1D ^1H NMR. 150 μL of the reaction mixture (0.75 mM substrate, 20 mM HEPES, 10 mM, pH 7.5, 75 mM NaCl, 25 μM protein) was diluted with 450 μL of D_2O. ^1H NMR (600 MHz): 8.42 ppm, s (1H); 8.11 ppm, d (1H), $^3J = 8$ Hz; 6.49 ppm, d (1H), $^3J = 8$ Hz.

1. Shen Y, Atreya HS, Liu G, Szyperski T (2005) G-matrix Fourier transform NOESY-based protocol for high-quality protein structure determination. *J Am Chem Soc* 127:9085–9099.
2. Kanelis V, Forman-Kay JD, Kay LE (2001) Multidimensional NMR methods for protein structure determination. *IUBMB Life* 52:291–302.
3. Ottiger M, Delaglio F, Bax A (1998) Measurement of J and dipolar couplings from simplified two-dimensional NMR spectra. *J Magn Reson* 131:373–378.
4. Hansen MR, Mueller L, Pardi A (1998) Tunable alignment of macromolecules by filamentous phage yields dipolar coupling interactions. *Nat Struct Biol* 5:1065–1074.
5. Delaglio F, et al. (1995) NMRPipe: A multidimensional spectral processing system based on UNIX pipes. *J Biomol NMR* 6:277–293.
6. Bartels C, Xia T-H, Billeter M, Güntert P, Wüthrich K (1995) The program XEASY for computer-supported NMR spectral analysis of biological macromolecules. *J Biomol NMR* 6:1–10.
7. Ulrich EL, et al. (2008) BioMagResBank. *Nucleic Acids Res* 36:D402–4088.
8. Shen Y, Delaglio F, Cornilescu G, Bax A (2009) TALOS+: A hybrid method for predicting protein backbone torsion angles from NMR chemical shifts. *J Biomol NMR* 44:213–223.
9. Herrmann T, Güntert P, Wüthrich K (2002) Protein NMR structure determination with automated NOE assignment using the new software CANDID and the torsion angle dynamics algorithm DYANA. *J Mol Biol* 319:209–227.
10. Chattopadhyaya R, Meador WE, Means AR, Quiocho FA (1992) Calmodulin structure refined at 1.7 Å resolution. *J Mol Biol* 228:1177–1192.
11. Schwieters CD, Kuszewski JJ, Tjandra N, Clore GM (2003) The Xplor-NIH NMR molecular structure determination package. *J Magn Reson* 160:65–73.
12. Zweckstetter M, Bax A (2000) Prediction of sterically induced alignment in a dilute liquid crystalline phase: Aid to protein structure determination by NMR. *J Am Chem Soc* 122:3791–3792.
13. Laskowski RA, Rullmannn JA, MacArthur MW, Kaptein R, Thornton JM (1996) AQUA and PROCHECK-NMR: Programs for checking the quality of protein structures solved by NMR. *J Biomol NMR* 8:477–486.
14. Word JM, Bateman RC Jr., Presley BK, Lovell SC, Richardson DC (2000) Exploring steric constraints on protein mutations using MAGE/PROBE. *Protein Sci* 9:2251–2259.
15. Huang YJ, Powers R, Montelione GT (2005) Protein NMR recall, precision, and F-measure scores (RPF scores): Structure quality assessment measures based on information retrieval statistics. *J Am Chem Soc* 127:1665–1674.
16. Wilson MA, Brunger AT (2000) The 1.0 Å crystal structure of Ca^{2+}-bound calmodulin: An analysis of disorder and implications for functionally relevant plasticity. *J Mol Biol* 301:1237–1256.
17. Olsson LL, Sjolin L (2001) Structure of *Escherichia coli* fragment TR2C from calmodulin to 1.7 Å resolution. *Acta Cryst Sect D* 57:664–669.
18. Finn BE, et al. (1995) Calcium-induced structural changes and domain autonomy in calmodulin. *Nat Struct Biol* 2:777–783.
19. Ishida H, Huang H, Yamniuk AP, Takaya Y, Vogel HJ (2008) The solution structures of two soybean calmodulin isoforms provide a structural basis for their selective target activation properties. *J Biol Chem* 283:14619–14628.

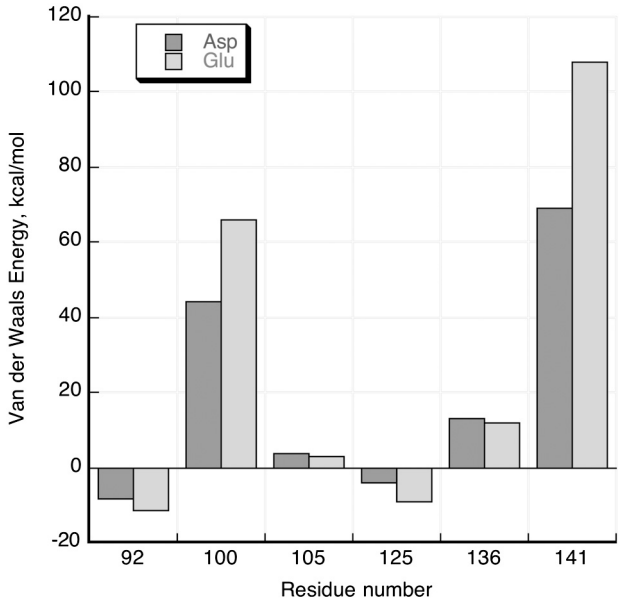

Fig. S1. Van der Waals energies of Asp and Glu mutants in the lowest energy rotamers at the residues that line the hydrophobic pocket of cCaM. Only positions 92, 105, and 125 can accommodate the carboxylates.

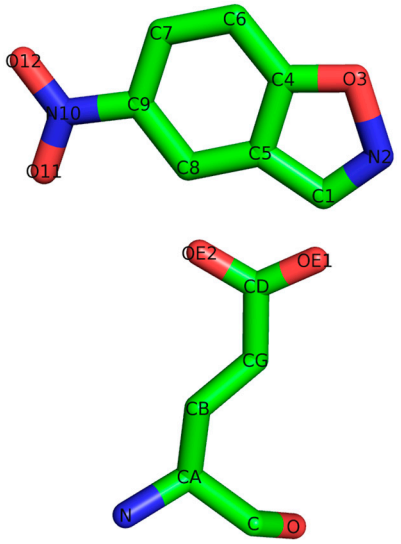

Fig. S2. Superrotamer geometry for Glutamate-5-nitrobenzisoxazole. Distances: OE1-C1 2.930 Å; angles: CD-OE1-C1 120°; OE1-C1-N2 131.010°; OE1-C1-C5 120.833°; dihedral angles: CD-OE1-C1-N2 180°; CD-OE1-C1-C5 0°.

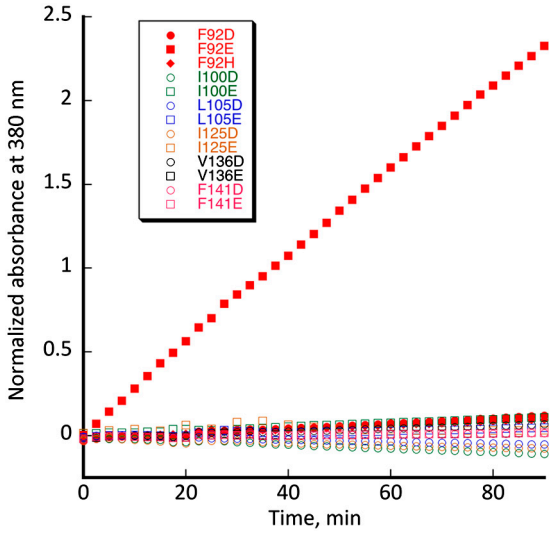

Fig. S3. Initial screening of calmodulin mutants for Kemp elimination activity. Conditions: 15 μM of protein, 0.5 mM substrate, 20 mM HEPES (pH 6.9); 150 mM NaCl, 10 mM $CaCl_2$.

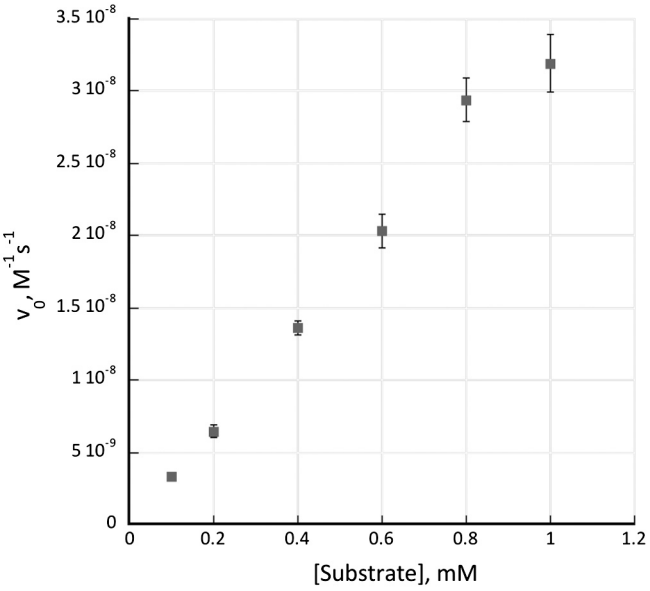

Fig. S4. The concentration dependence of the initial rate of Kemp elimination for AlleyCat.

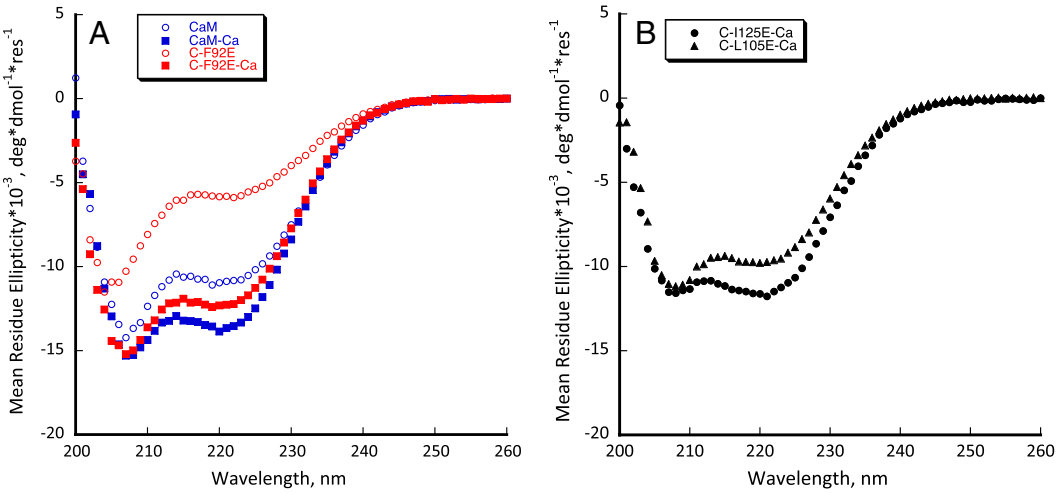

Fig. S5. (*A*) CD spectra of the wild-type cCaM (blue) and AlleyCat (red). Conditions: 3 mM HEPES, pH 7.0; 30 mM NaCl; 25 μM protein, 0.5 mM $CaCl_2$. (*B*) CD spectra of cCaM L105E (triangles) and cCaM I125E (circles). Conditions: 4 mM HEPES, pH 6.9; 30 mM NaCl; 25 μM protein (I125E), 40 μM protein (L105E); 2 mM $CaCl_2$. CD measurements were done on a Jasco J-810 circular dichroism spectrometer using 1 mm pathlength quartz cuvettes.

Table S1. Energies calculated for the Glutamate-5-nitrobenzisoxazole superrotamers in positions F92, I105, and I125 compared to the energies of mutants

Mutant	van der Waals energy, kcal/mol	Electrostatic energy, kcal/mol
F92D	−8.40917	−0.24903
F92E	−11.41357	−0.14955
F92E-superrotamer	17.47396	−7.19485
L105D	3.64222	−0.34728
L105E	2.95244	−0.21339
L105E-superrotamer	240.42016	−7.18744
I125D	−4.42834	−0.23240
I125E	−8.84581	−0.21975
I125E-superrotamer	154.35296	−7.51254

A small clash that could be removed by minimization was observed in the F92E-superrotamer. However, superrotamers of L105E and I125E could not accommodate the substrate in the binding pocket.

Table S2. NMR and refinement statistics for AlleyCat

	AlleyCat
NMR distance and dihedral constraints	
Distance constraints	
Total NOE	1205
Intraresidue	359
Interresidue	846
Sequential ($\|i - j\| = 1$)	305
Medium-range ($\|i - j\| < 4$)	270
Long-range ($\|i - j > 5$)	271
Intermolecular	0
Hydrogen bonds	0
Total dihedral angle restraints	140
Phi	70
Psi	70
Structure statistics	
Violations (mean and s.d.)	
Distance constraints (>0.5 Å)	0.2 ± 0.4
Dihedral angle constraints (>5°)	0.3 ± 0.7
Max. dihedral angle violation (°)	8.6
Max. distance constraint violation (Å)	0.54
Deviations from idealized geometry	
Bond lengths (Å)	0.0018 ± 0.0004
Bond angles (°)	0.36 ± 0.01
Impropers (°)	0.29 ± 0.03
Average pairwise rmsd* (Å)	
Heavy	1.62 ± 0.15
Backbone	0.76 ± 0.21

*Pairwise rmsd was calculated among 20 refined structures.
Total RDCs; 50, Q (%) for all 50 RDCs; 10.6 ± 1.9, Q_{free} (%) for unused 10 RDCs; 21.8 ± 5.0.

Table S3. Additional structure statistics for NMR structure of AlleyCat

Average number of constraints per residue	16.2
Average number of long-range distance constraints per residue	3.1
Average rmsd to the mean coordinates [Å]	
Regular secondary structure elements *, backbone heavy atoms	0.48 ± 0.17
Regular secondary structure elements *, all heavy atoms	1.14 ± 0.12
Ordered residues †, backbone heavy atoms	1.05 ± 1.02
Ordered residues †, all heavy atoms	1.59 ± 0.99
Heavy atoms of molecular core including best-defined side chains ‡	0.70 ± 0.09
PROCHECK (13) G-factors raw score (ϕ and ψ / all dihedral angles) †	0.48/0.33
PROCHECK (13) G-factors Z score (ϕ and ψ / all dihedral angles) †	2.20/1.95
MOLPROBITY (14) clash score (raw / Z score) †	23.58/ − 2.52
AutoQF R/P/DP scores (15) [%]	96/93/78

*Residues 82–92, 99–112, 118–128, 135–146 (not including 69–76)
†Residues 69–76, 82–96, 99–112, 114–147.
‡Backbone and side chain heavy atoms of residues 85, 88–89, 91, 93, 97, 100–105, 108, 110, 112, 116–117, 121–122, 125, 128–131, 133, 136, 140, 141, 142.